OE Optical Engineering

RESEARCH PAPER

Development of thin film quarter-waveplate for polarization-independent liquid crystal on silicon phase modulators

Isaac Zachmann,* Anastasiia Svanidze, Qirui Zhang, Lianhua Ji, Kristina Johnson, and Chongchang Mao

The Ohio State University, Electroscience Laboratory, Department of Electrical and Computer Engineering, Columbus, Ohio, United States

ABSTRACT. Liquid crystal on silicon (LCoS) phase modulators spatially modulate the phase of light across the panel. The orientation order and elongated molecules of nematic liquid crystals (LCs) means that traditional LCoS phase modulators are inherently polarization-dependent, resulting in either complicated polarization manipulation systems or high optical power loss for unpolarized incident light. We propose a polarization-independent LCoS (PI-LCoS) device that combines existing technologies, which allows for cost-effective fabrication. Our PI-LCoS phase modulator is suitable for a wide variety of applications in telecommunication, adaptive optics, and display technologies. We have demonstrated the feasibility of the proposed PI-LCoS device by fabricating polarization-independent LC cells using a thin-film quarter-wave plate composed of a photoalignment layer and a layer of LC polymer. We show experimentally that the proposed design can efficiently modulate the phase of light with arbitrary input polarization.

Keywords: liquid crystal on silicon; spatial light modulator; adaptive optics; polarization management; quarter-wave plate

Paper 20230202G received Mar. 3, 2023; revised May 16, 2023; accepted Jun. 9, 2023; published Jun. 23, 2023.

1 Introduction

Phase-only liquid crystal on silicon (LCoS) devices are used in a variety of applications including wavelength selective switches (WSS),[1] wavefront correction for optical communications and astronomical observation, and holographic displays for augmented reality/virtual reality (AR/VR).[2] Since current LCoS devices only modulate a single polarization, they require significant polarization management optics which make the system larger, more expensive, and less efficient.[2] A necessary improvement is to make LCoS devices polarization-independent, which would reduce cost, size, and complexity of systems while increasing system performance.

As shown in Fig. 1, a typical LCoS phase modulator consists of a silicon backplane circuit with a two-dimensional array of electrically addressable pixels and a glass substrate with a transparent electrode. A liquid crystal (LC) alignment layer is applied to each substrate to pre-align LC molecules, and a layer of LC is sandwiched between the two substrates. By varying the voltage across the LC layer, the effective refractive index for light propagating through the device can be locally changed for the polarization parallel to the pre-alignment direction. Since each pixel on the silicon backplane can be supplied with a defined voltage, light is spatially phase

*Address all correspondence to Isaac Zachmann, zachmann.4@osu.edu

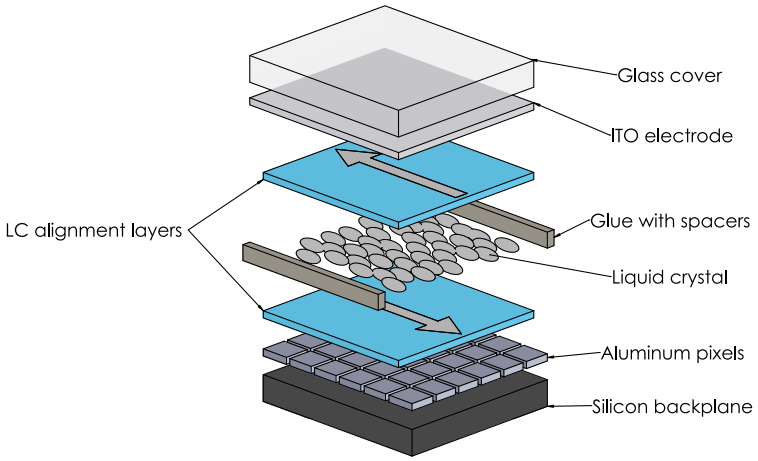

Fig. 1 Structure of a traditional LCoS phase modulator.

modulated as it passes through the LC layer, reflects off the pixel mirrors, and again passes through the LC layer. For this type of LCoS device, phase modulation will only occur for the light polarized parallel to the LC pre-alignment direction, since the light that is polarized orthogonally to the alignment direction is always subjected to the ordinary refractive index of the LC, regardless of the applied voltage. LCoS devices used in applications, such as WSS, wavefront correction, or holographic display, require a significant degree of polarization management or, if using only a single polarization, are characterized by high optical power loss. Given these significant deficiencies inherent in single polarization modulation, the development of polarization-independent LCoS (PI-LCoS) phase modulators has attracted both industry and academia. Frisken et al.[3] outlined many of the proposed methods for making PI-LCoS devices. One concept for fabricating PI-LCoS devices involves using two LC layers that are orthogonally pre-aligned and modulated together.[4] In this configuration, a single LC layer modulates one input polarization, and the other LC layer modulates the orthogonal polarization. Since any input polarization can be represented by the superposition of these two orthogonal polarizations, the device has the same modulation for light with any polarization resulting in polarization-independent modulation. Using two LC layers in one device, however, requires a higher driving voltage for the same phase delay since the glass electrode is further from the pixel array. Additionally, it is difficult to configure equal phase delay at every pixel for both layers. Rather than using two LC layers, another method proposes making a PI-LCoS device using axially symmetric LCs, but this technology is immature.[3]

A simple method to realize polarization-independent LC devices is to rotate each polarization of light by 90 deg after the first pass through the LC layer. When the light passes through the LC layer a second time, the polarization that was originally modulated by the LCs is now perpendicular to the LC alignment direction and receives no further modulation. At the same time, the polarization that was originally orthogonal to the LC alignment direction on the first pass is now parallel to the LC alignment direction and is modulated by the LC layer. This method of creating polarization-independent LC devices is well developed and widely understood.[5]

One of the simplest methods to achieve the polarization rotation in LC devices is to add a quarter-wave plate (QWP) between the LC layer and the mirror.[5] Adding a traditional crystal waveplate to an LCoS device, however, is not feasible since the thickness of the waveplate would greatly increase the distance between the electrodes, which means that a significantly higher driving voltage would be required to modulate the LCs.

Frisken et al.[3] proposed to fabricate a subwavelength grating on each pixel to achieve the polarization rotation. The grating would be composed of alternating metal and dielectric strips that act as birefringent material when the strips are smaller than the wavelength of light. This method of realizing the polarization rotation is advantageous in that the voltage drop over the grating is very low, since it is made partially of a conductive metal. Therefore, no significantly higher voltages are required to drive the LC layer. The major disadvantage of this method, however, is the difficulty in fabricating high-quality gratings on the LCoS backplane with low cost

and high efficiency. In an attempt to simplify the grating fabrication, Anderson et al.[6] proposed adding a dielectric spacer layer between the pixel array and grating. Even with a simplified fabrication process, however, it is difficult to achieve high efficiency polarization-independent phase-modulation using such subwavelength gratings on the silicon backplane surface.

2 PI-LCoS Structure and Operation

We propose a practical PI-LCoS phase modulator, as shown in Fig. 2, which uses a thin-film polymer QWP and uses a frame buffer pixel circuit for the silicon backplane to increase the driving voltage.[7] The significant advantages of this method are that existing silicon chip fabrication processes can be used for the backplane and thin-film polymer waveplate fabrication is a relatively simple process.[8,9] Therefore, it is highly possible to realize low-cost and high-performance PI-LCoS phase modulators. Here we focus on developing a PI-LCoS device for visible light (633 nm), however, the same methods will be used in the future to fabricate PI-LCoS devices that operate in infrared wavelengths (1550 nm). Fabricating the PI-LCoS device will be slightly more difficult for infrared wavelengths as the QWP and LC layers will need to be thicker due to the physically longer wavelength and dispersion, but the methodology and process are the same for both infrared and visible wavelengths. For our PI-LCoS device, the LC layer's thickness should allow for 2π modulation in a single pass since each polarization state is modulated one time. This differs from traditional LCoS devices, where the single polarization state is modulated 2 times.

The focus of this paper is the development of thin-film polymer waveplate fabrication techniques for use in our PI-LCoS devices. The polymer QWP is fabricated using a layer of photoalignment material to set the optical axis and a layer of liquid crystal polymer (LCP), which acts as the birefringent medium.[9] The thickness of the LCP layer depends on the operating wavelength and the specific LCP material, but using LCP materials with high birefringence, we can achieve a thin QWP with a low-voltage drop. Therefore, we are exploring LCP materials with high birefringence.

Instead of increasing the voltage to the pixels directly, the frame buffer pixel circuit allows us to use V_{com} modulation to increase the voltage across the LC layer.[8,10] In general, an alternating current (AC) driving scheme is used in LC phase modulators to prevent the degradation of the LC layer due to charged particles being pulled to one electrode. In traditional LCoS devices, this AC driving is achieved by holding the common voltage on the glass electrode V_{com} at a mid-voltage between the maximum and minimum voltages supplied by the silicon backplane. By modulating V_{com} opposite to the pixel mirrors, as described in Ref. 10, we increase the voltage across the LC layer. This V_{com} modulation is possible because the frame buffer pixel technology updates all

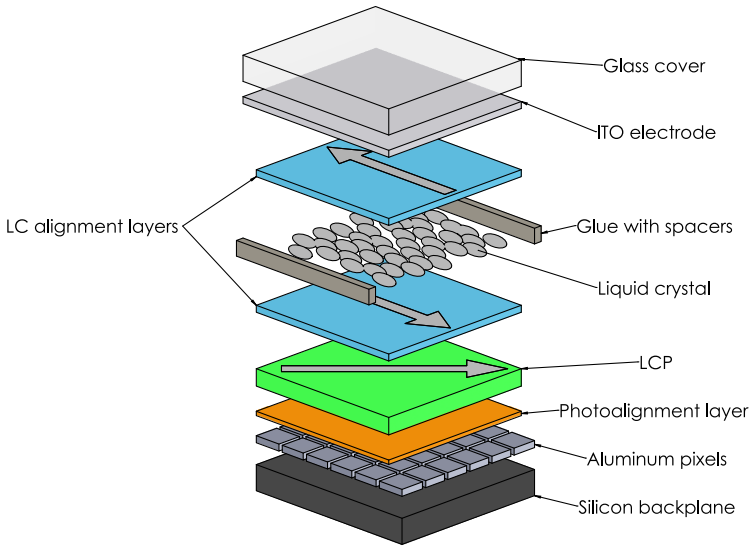

Fig. 2 Structure of the proposed PI-LCoS phase modulator.

pixels simultaneously instead of line by line. We have begun the fabrication process for our first frame buffer pixel silicon backplane design which will be used to demonstrate 64×64 pixel PI-LCoS phase modulators with up to 2π modulation for visible light. For this first backplane, the pixels are 5 μm squares with a pitch of 8 μm.

Our proposed PI-LCoS devices have major advantages compared to traditional LCoS devices for specific applications in WSS, wavefront correction, and holographic display. In telecommunication systems that use WSS, the input light does not have a specified polarization. The polarization-independent operation of our proposed LCoS device eliminates the need for polarization management optics, such as a polarizing beamsplitter and a half-wave plate which would be required if using a traditional LCoS modulator. These optics increase system complexity and are difficult to align, leading to higher polarization-dependent loss. In wavefront correction, a traditional LCoS modulator would require the polarization management optics to be even larger and more complex than WSS applications due to the large diameter of the input beam (e.g., light coming from a telescope for astronomical imaging). Our PI-LCoS modulator eliminates this problem by removing the polarization management altogether. Also our PI-LCoS phase modulator can perform frame at a time wavefront correction that can significantly improve image quality and light efficiency. For holographic display, the frame buffer pixel circuit has major advantages of high image display quality and high light efficiency. This is critically important for color sequential display, because red, green, and blue images need to be displayed with high frame rate and time sequentially. Using a traditional LCoS phase modulator for such display, the light needs to be blocked during data loading time, resulting in low light efficiency. With our frame buffer pixel circuits based LCoS phase modulator, data loading and display can be done in parallel, which can significantly improve the light efficiency compared to traditional LCoS phase modulators.

3 QWP Development

The QWP is fabricated from two layers, both of which are applied to the substrate via spin coating. The first layer is a thin (10 to 50 nm) photoalignment layer which is made of a material with molecules that are aligned by polarized light. The second layer is thicker (0.5 to 3 μm) and made of a birefringent LCP. Intermolecular forces align the LCP molecules parallel to the photoalignment molecules which sets the optical axis of the QWP. To fabricate the QWP, we selected materials that are widely used in research and are commercially available.

3.1 Materials

For the photoalignment material, we used brilliant yellow (BY) provided by Sigma Aldrich. When exposed to polarized ultra-violet (UV) light, the BY molecules oriented along the direction of polarization will absorb light and rotate. The molecules that are perpendicular to the input polarization do not absorb light and do not rotate. After sufficient exposure, all the BY molecules assume an orientation that is perpendicular to the polarization of incident light. Intermolecular forces then lock the BY molecules in place once this perpendicular alignment is achieved.[11]

For the LCP material, we used RM257 from Synthon. The elongated structure of RM257 molecules makes them birefringent, which is critical for QWP fabrication. The birefringence of RM257 for visible light is $\Delta n = 0.179$ ($n_e = 1.687$ and $n_o = 1.508$).[12] Thus for a wavelength of 633 nm, a QWP composed of RM257 should be 884 nm thick.

Spin coating a uniform layer of material with reproducible thickness requires first dissolving the material in a solvent. As suggested by Wang et al.,[13] we found that dimethylformamide was a good solvent for BY. For the mixture of RM257 and I-651, we used toluene as the solvent.

3.2 QWP Fabrication

The QWP was fabricated on an aluminum-coated silicon substrate, which reflects light and acts as an electrode for LC modulation. First, the BY mixture was spin coated onto the substrate. After spin coating, the BY layer was dried on a hotplate to evaporate any residual solvent, then exposed to polarized UV light.

Once the photoalignment layer was fabricated, the LCP mixture was spin coated on top of the photoalignment layer. The sample was then immediately placed into a nitrogen-rich

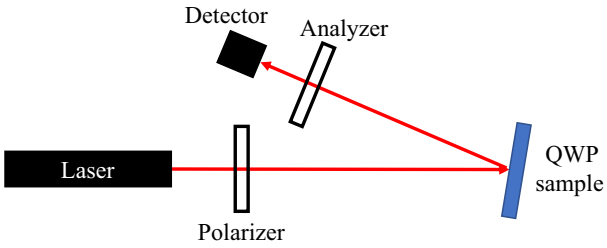

Fig. 3 Measurement setup used to test QWP effectiveness.

environment and exposed with unpolarized UV light. By adjusting the LCP concentration in solvent, spin coating speed, and spin time, we successfully developed a two-step coating process to reach the desired QWP thickness.

3.3 Testing

Here we fabricated several QWPs using our developed process and performed waveplate measurements. When developing PI-LCoS devices, it is important to consistently fabricate QWPs with the correct thickness. Therefore, we first measured the samples using an ellipsometer, which takes polarization measurements at many wavelengths and fits the data to a model. Next, we used an optical setup to measure the polarization change induced by the QWP.

The ellipsometer data showed that the thickness of the LCP layer was consistently within 10% deviation of the 884 nm target thickness, and that multiple samples were within 5% deviation of the desired thickness. We will further develop the QWP fabrication process to reduce the thickness error.

The optical setup used to measure the QWP is shown in Fig. 3. In the setup, the beam from a 633 nm HeNe laser first passes through a linear polarizer and is incident on the sample at a small incident angle. The reflected beam then passes through a second linear polarizer, known as the analyzer, and the output power is measured with a photodetector and a power meter. The orientation of the optical axis of the sample is 45 deg from the input polarization. In the ideal case, after the light passes through the QWP twice, the polarization is rotated by exactly 90 deg. Therefore, when the two polarizers are in parallel orientations, very little power should transmit, and when the polarizers are in perpendicular orientations, very high-power should transmit. The ratio of these two measured powers can be used to quantify how effectively the QWP rotates the polarization of light. Here the measured optical power passed through crossed polarizers was typically 10 times the optical power passed through parallel polarizers. These measurements indicate that a double pass through the QWP was effective at rotating the polarization of light by 90 deg.

4 Polarization-Independent Liquid Crystal Cell

After developing the QWP fabrication process, we fabricated and tested a polarization-independent liquid crystal (PI-LC) cell, the structure of which is similar to the PI-LCoS shown in Fig. 2. The PI-LC cell operates upon the same principles as our proposed LCoS device and includes all the same layers as the PI-LCoS device, but instead of a silicon backplane circuit with individually addressable pixels, we used a silicon substrate with a single aluminum layer. Thus the device demonstrates how a single pixel of the PI-LCoS device produces polarization-independent phase modulation.

4.1 Materials

For the LC alignment layers, we used commercially available polyvinyl alcohol (PVA) from Sigma Aldrich, as it is widely used in research. To prepare the PVA for spin coating, it was dissolved in 80°C deionized water. To set the alignment direction of PVA, the thin PVA film was rubbed with a velvet cloth.

For the LC material, we used E7 LC, which has a birefringence of 0.2 for visible light.[14] For the wavelength of 633 nm, 2π phase modulation requires a minimum LC layer thickness of 3.2 μm. To achieve a uniform layer with this minimum thickness, we used 3.34-μm silicon

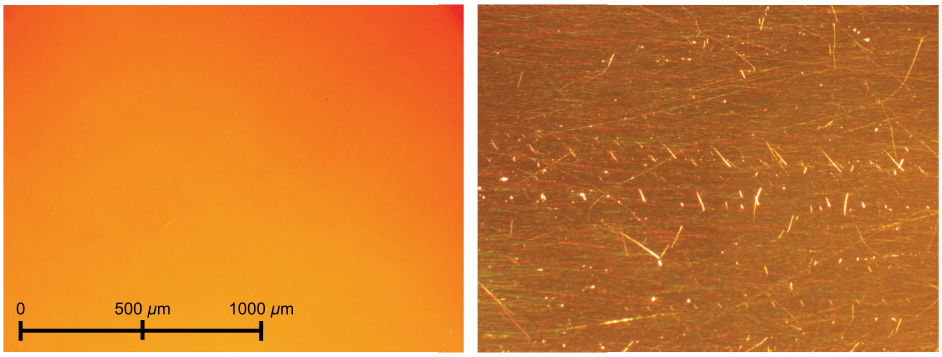

Fig. 4 Microscope images of a fabricated PI-LC cell through crossed polarizers. (a) Incident light is polarized parallel to LC alignment and 45 deg from QWP optical axis. (b) Incident light is polarized 45 deg from LC alignment and parallel to QWP optical axis.

spacers, which were mixed with Norland optical adhesive 86H that was used to glue the cell together.

4.2 Cell Assembly

The first step in PI-LC cell assembly was to fabricate a polymer QWP on an aluminum layer as discussed in Sec. 3.2. Next, the PVA alignment layer was spin coated onto the QWP and rubbed with a velvet cloth to set the alignment direction. Another alignment layer was then fabricated on a glass substrate with an idium tin oxide (ITO) electrode. Once the alignment layers were fabricated, the two substrates were glued together with their rubbing directions oriented in an antiparallel direction. The glue was then cured with UV light. Once assembled, the cell was filled with the E7 LC using capillary action. Finally, conductive epoxy was used to attach wires to the aluminum and ITO electrodes.

5 Results

The fabricated PI-LC cells were viewed through cross polarizers under a microscope. Images of a PI-LC cell, shown in Fig. 4, demonstrate uniform LC alignment with only minor defects from rubbing. After fabricating the PI-LC cell, we used an interferometer to measure the phase modulation as a function of applied voltage for various input polarizations, along with the device transmittance for various input polarizations in order to calculate the polarization-dependent loss (PDL).

5.1 Interference Measurement

To demonstrate the polarization-independent operation, we measured phase modulation for various input polarizations using the interferometer setup shown in Fig. 5. Here a crystal polarizer and a half wave plate set the polarization of input light. A beamsplitter is then used to create two

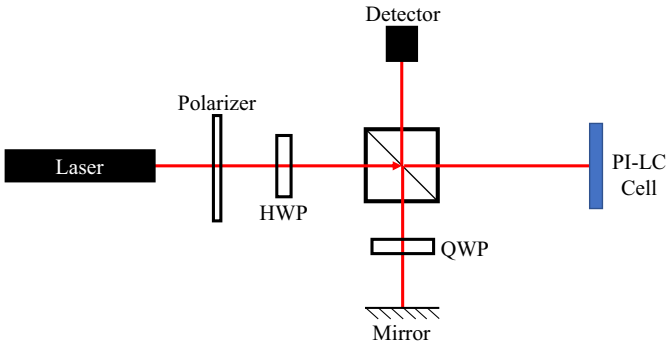

Fig. 5 Measurement setup used to test phase modulation.

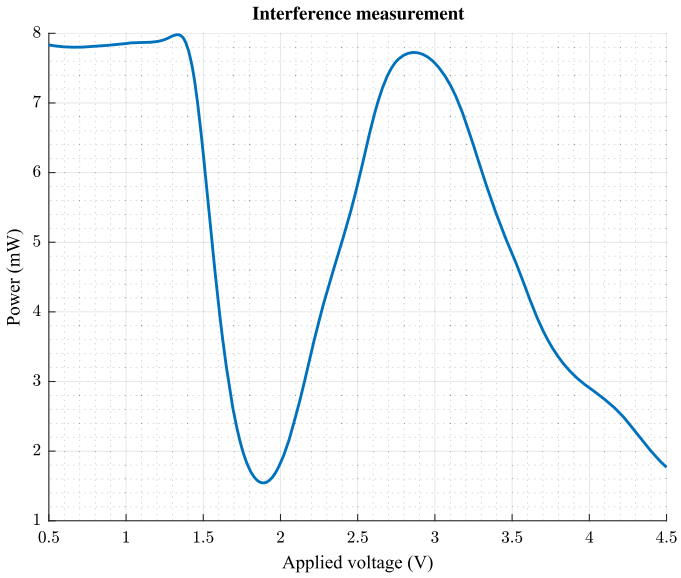

Fig. 6 Power measured at the output of the interferometer as a function of voltage applied to the PI-LC cell for input polarization 90 deg from LC alignment direction.

beams. The first (object beam) goes to the PI-LC cell and is phase modulated by the device; the second (reference beam) passes through a QWP and is reflected back to the beamsplitter. The QWP in the reference beam path compensates for the polarization change caused by the QWP in the PI-LC cell. This way, when interference is measured at the output of the interferometer, the polarization of the reference beam matches the polarization of the object beam. Various voltages are applied to the PI-LC cell using a function generator. The power detector is connected to a power meter which is connected to an oscilloscope to record the data. A curve showing the applied voltage to the cell versus the power output of the interferometer is shown in Fig. 6 for a single polarization. Here we see that as the applied voltage increases, the interferometer shifts between constructive and destructive interference due to the phase change induced by the cell.

The HWP was rotated to five positions to create five unique input polarizations. For each of these polarizations, the power at the detector was measured as a function of voltage applied to the cell. Additionally, the power of the reference beam was measured by blocking the object beam, and the power of the object beam was measured by blocking the reference beam. These measurements were then used to calculate the phase delay of the object beam as a function of voltage.

The power of two interfering waves with powers P_1 and P_2 can be expressed by

$$P = P_1 + P_2 + 2\sqrt{P_1 P_2}\cos(\phi), \tag{1}$$

where ϕ is the phase difference between the two waves. In practice, there is always some misalignment between the beams. Additionally, the fabricated QWP has non-ideal alignment and thickness so there is some component of the polarization that is not rotated by 90 deg. The absence of the same polarization component in the reference beam prevents interference of this unrotated light. To account for light that does not interfere due to either QWP quality or beam misalignment, we include a factor C in Eq. (1) to obtain

$$P_V = P_1 + P_2 + 2C\sqrt{P_1 P_2}\cos(\phi_V), \tag{2}$$

where C assumes a value between 0 (no interference) and 1 (ideal interference). Here the measured power of the reference beam is P_1, the measured power of the object beam is P_2, the measured power of the interfering beams is P_V, and the phase difference between the two beams is ϕ_V. The subscript V indicates the variables that are a function of applied voltage. Rearranging Eq. (2), we obtain

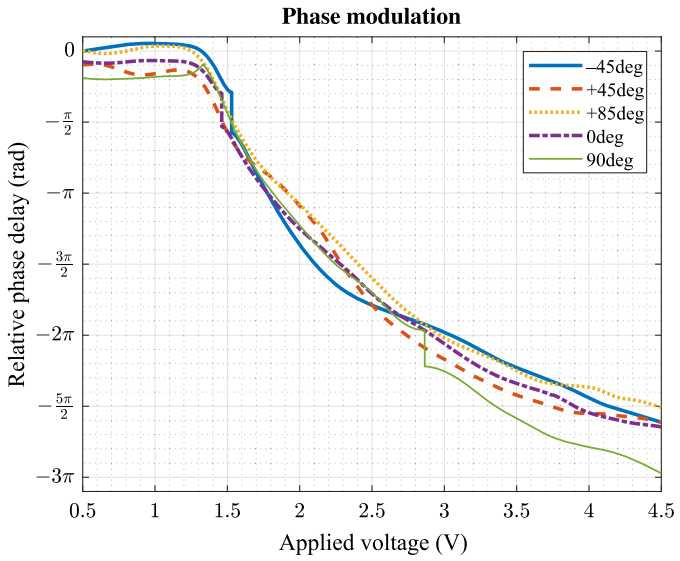

Fig. 7 Phase modulation as a function of applied voltages for various input polarizations. The legend shows the angle between the input polarization and the LC pre-alignment direction.

$$\cos(\phi_V) = \frac{P_V - P_1 - P_2}{2C\sqrt{P_1 P_2}}. \tag{3}$$

Here we see that ϕ_V is ambiguous, and C is unknown. From the operational theory of the device, we know that ϕ_V should be a continuous function of applied voltage spanning at least 2π and, in general, decrease as the applied voltage increases. We can then assume that $\cos(\phi_V)$ varies between -1 and 1 and thus find a value for C along with an offset to apply to the right side of Eq. (3) so that it spans -1 to 1. After applying the scaling and offset, we can compute ϕ_V. Since ϕ_V is in the argument of cosine, the specific value of ϕ_V is ambiguous, so we choose values such that ϕ_V decreases as the applied voltage increases.

Note the similarity of the phase modulations for the various input polarizations in Fig. 7, as well as the computed value for C that is close to 0.75 in all cases. Differences in phase modulation curves may be attributed to a number of measurement errors, such as physical motion in the interferometer or variation in the optical power of the laser between measurements. The results indicate that a similar amount of light is modulated, regardless of input polarization; hence the device is polarization-independent.

5.2 Polarization-Dependent Loss

For PI-LCoS devices developed in the future, an important device specification will be the PDL. The PDL, in dB, is defined by the following equation:

$$\mathrm{PDL} = 10\log_{10}\frac{T_{\max}}{T_{\min}}. \tag{4}$$

Here $T_{\max}$ and $T_{\min}$ are the maximum and minimum transmission values as a function of input polarization. We should note that these transmission values do not depend on the output polarization. Although it is possible to determine $T_{\max}$ and $T_{\min}$ by measuring transmission for every possible input polarization, this measurement would be extremely time-consuming. Instead, we can measure transmission at just four polarizations to determine an equation for transmission as a function of input polarization. Once this equation is known, the maximum power and minimum power can be used to determine $T_{\max}$ and $T_{\min}$.

To compute PDL, we use Mueller calculus to first find an expression for transmission as a function of input polarization.[15] Specifically, since the first row of the Mueller matrix fully describes the output power of a system, the first row of the Muller matrix of the device is computed. Since the first row has four free parameters, a minimum of four measurements is required. Going beyond Ref. 15, in which exactly four measurements are taken, we show that a least

squares solution can be computed using any number of measurements greater than four. By taking more measurements, we can reduce error.

The four stokes parameters ($S0$, $S1$, $S2$, and $S3$) are used to represent the intensity, polarization, and degree of polarization of a monochromatic source. $S0$ is the only stokes parameter needed to describe the output intensity of a system given the input stokes vector. Thus the transmission can be computed for any arbitrary input light if the first row of the Mueller matrix is known. Using this fact, we can develop the following matrix relationship:

$$\begin{bmatrix} S0_{\text{out}\,1} \\ S0_{\text{out}\,2} \\ \vdots \\ S0_{\text{out}\,N} \end{bmatrix} = \begin{bmatrix} S0_{\text{in}\,1} & S1_{\text{in}\,1} & S2_{\text{in}\,1} & S3_{\text{in}\,1} \\ S0_{\text{in}\,2} & S1_{\text{in}2} & S2_{\text{in}2} & S3_{\text{in}\,2} \\ \vdots & \vdots & \vdots & \vdots \\ S0_{\text{in}\,N} & S1_{\text{in}\,N} & S2_{\text{in}\,N} & S3_{\text{in}\,N} \end{bmatrix} \begin{bmatrix} m_{11} \\ m_{12} \\ m_{13} \\ m_{14} \end{bmatrix}. \tag{5}$$

Here $SX_{\text{in}\,M}$ is the X'th stokes parameter of the input light on the M'th measurement, and $S0_{\text{out}\,M}$ is the intensity of the output on the M'th measurement. The value m_{ij} is the element of the Mueller matrix appearing in the i'th row and j'th column. Using this matrix equation, we can compute a least squares estimation for the first row of the Mueller matrix given N measurements. For each measurement, the input polarization and output intensity are determined by controlling the input polarization and measuring the intensity with a power detector. If we define

$$y = \begin{bmatrix} S0_{\text{out}\,1} \\ S0_{\text{out}\,2} \\ \vdots \\ S0_{\text{out}\,N} \end{bmatrix}; \quad A = \begin{bmatrix} S0_{\text{in}\,1} & S1_{\text{in}\,1} & S2_{\text{in}\,1} & S3_{\text{in}\,1} \\ S0_{\text{in}\,2} & S1_{\text{in}\,2} & S2_{\text{in}\,2} & S3_{\text{in}\,2} \\ \vdots & \vdots & \vdots & \vdots \\ S0_{\text{in}\,N} & S1_{\text{in}\,N} & S2_{\text{in}\,N} & S3_{\text{in}\,N} \end{bmatrix}; \quad x = \begin{bmatrix} m_{11} \\ m_{12} \\ m_{13} \\ m_{14} \end{bmatrix}, \tag{6}$$

then the least squares solution for x is

$$x = (A^{\text{T}}A)^{-1}A^{\text{T}}y. \tag{7}$$

The result is a least-squares estimate for the first row of the Mueller matrix. Once the values for the first row of the Mueller matrix are determined, we can solve for the maximum and minimum transmission values using the equations from Ref. 15:

$$T_{\text{max}} = m_{11} + \sqrt{m_{12}^2 + m_{13}^2 + m_{14}^2}, \tag{8}$$

$$T_{\text{min}} = m_{11} - \sqrt{m_{12}^2 + m_{13}^2 + m_{14}^2}. \tag{9}$$

These values are then used in Eq. (4) to compute the PDL of a device. To measure the PDL of our device, we used different five input polarizations generated by combining a linear polarizer and a transparent QWP. These polarizations are described by five stokes vectors: linear horizontal, linear vertical, linear 45 deg, right-handed circular, and left-handed circular, respectively, as follows:

$$\begin{bmatrix} P_{\text{in}} \\ P_{\text{in}} \\ 0 \\ 0 \end{bmatrix}, \begin{bmatrix} P_{\text{in}} \\ -P_{\text{in}} \\ 0 \\ 0 \end{bmatrix}, \begin{bmatrix} P_{\text{in}} \\ 0 \\ P_{\text{in}} \\ 0 \end{bmatrix}, \begin{bmatrix} P_{\text{in}} \\ 0 \\ 0 \\ P_{\text{in}} \end{bmatrix}, \begin{bmatrix} P_{\text{in}} \\ 0 \\ 0 \\ -P_{\text{in}} \end{bmatrix}. \tag{10}$$

Here P_{in} is the power incident on the device. We measured the output power after the light is reflected from the PI-LC cell. Using these measurements, we found $T_{\text{max}} = 77\%$ and $T_{\text{min}} = 70\%$, which results in 0.4 dB PDL. We expect to further improve the QWP fabrication process to reduce the PDL of the device.

6 Conclusion

We proposed a PI-LCoS phase modulator that uses thin film QWP technology and frame buffer pixel circuit technology. Unlike traditional LCoS phase modulators, our proposed PI-LCoS phase modulators have significant advantages for use in WSS for fiber networks, wavefront

correction for astronomical imaging and free space optical communications, computer-generated holographic display, color sequential display, and AR/VR displays. We demonstrated the feasibility of the proposed LCoS device by fabricating and testing PI-LC cells that demonstrate the polarization-insensitive operation of the device and provide experimental data which can be used to estimate the required driving voltages for future LCoS devices. Future research entails considering more materials to optimize the device. Near future research entails using our developed processes and techniques to fabricate PI-LCoS phase modulators after receiving the silicon backplane chips from the silicon foundry.

Code, Data, and Materials Availability

The collected and used to generate Fig. 7 along with QWP measurements and PDL measurements are available to download at https://buckeyemailosu-my.sharepoint.com/:f:/g/personal/zachmann_4_buckeyemail_osu_edu/Ei93pHg1E3pJpeuklrfaPDYB8b9dS36g7EXB5NvmCorUBw or by contacting the authors.

Acknowledgments

Funding for this work was provided as seed funding from the College of Engineering at The Ohio State University. The authors declare no conflicts of interest.

References

1. G. Baxter et al., "Highly programmable wavelength selective switch based on liquid crystal on silicon switching elements," in *Opt. Fiber Commun. Conf. and the Natl. Fiber Opt. Eng. Conf.*, Vol. 3 (2006).
2. Z. Zhang, Z. You, and D. Chu, "Fundamentals of phase-only liquid crystal on silicon (LCoS) devices," *Light: Sci. Appl.* **3**(10), e213 (2014).
3. S. J. Frisken, G. W. Baxter, and Q. Wu, "Polarization-independent LCoS device," US Patent 9,065,707 (2015).
4. Y.-H. Wu et al., "Axially-symmetric sheared polymer network liquid crystals," *Opt. Express* **13**(12), 4638–4644 (2005).
5. G. D. Love, "Liquid-crystal phase modulator for unpolarized light," *Appl. Opt.* **32**(13), 2222–2223 (1993).
6. K. Anderson et al., "Reflective LC devices including thin film metal grating," US Patent 9,588,374 (2017).
7. C. Mao, "Polarization insensitive liquid crystal on silicon (LCoS) phase modulators and related devices and methods," US Patent 11,442,314, Set. 13 (2022).
8. S. Lee, C. Mao, and K. M. Johnson, "A novel frame-buffering circuit for liquid crystal on silicon microdisplays," in *LEOS 2000. 2000 IEEE Annu. Meeting Conf. Proc. 13th Annu. Meeting. IEEE Lasers and Electro-Opt. Soc. 2000 Annu. Meeting (Cat. No. 00CH37080)*, IEEE, Vol. 1, pp. 121–122 (2000).
9. Y. Wu et al., "Stretchable and foldable waveplate based on liquid crystal polymer," *Appl. Phys. Lett.* **117**(26), 263301 (2020).
10. S. Tan and X. Sun, "P-1: generic design of silicon backplane for LCoS microdisplays," in *SID Symp. Digest of Tech. Pap.*, Vol. 33, pp. 200–203 (2002).
11. Y. Folwill et al., "A practical guide to versatile photoalignment of azobenzenes," *Liquid Cryst.* **48**(6), 862–872 (2021).
12. C.-K. Liu, W.-H. Chen, and K.-T. Cheng, "Asymmetrical polarization-dependent scattering and reflection in a sole cell of polymer network-90 twisted nematic liquid crystals," *Opt. Express* **25**(19), 22388–22403 (2017).
13. J. Wang et al., "Effects of humidity and surface on photoalignment of brilliant yellow," *Liquid Cryst.* **44**(5), 863–872 (2017).
14. J. Li et al., "Infrared refractive indices of liquid crystals," *J. Appl. Phys.* **97**(7), 073501 (2005).
15. C. Hentschel and S. Schmidt, "PDL measurements using the agilent 8169a polarization controller," Agilent Technologies product note, http://application-notes.digchip.com/018/18-27210.pdf (2002).

Isaac Zachmann received his BS degree in electrical engineering from The Ohio State University (OSU) in 2022 and is currently a PhD candidate in electrical engineering at OSU. He is a graduate research associate at the Electroscience Laboratory of The Ohio State University.

Chongchang Mao has been working in the industry and academia for more than 30 years. In recent years, he is focusing on the technology and product development in the fields of liquid crystal display, LCoS phase modulators, and optical telecommunication networks. He is now supervising researchers and graduate students on the PI-LCoS phase modulator technology development.

Biographies of the other authors are not available.